Biotechnology and Bioprocess Engineering 17: 377-384 (2012)
DOI 10.1007/s12257-011-0105-8

RESEARCH PAPER

Immobilization of Porcine Pancreatic α-amylase on Magnetic Fe_2O_3 Nanoparticles: Applications to the Hydrolysis of Starch

Mohammad Jahir Khan, Qayyum Husain, and Ameer Azam

Received: 13 March 2011 / Revised: 30 December 2011 / Accepted: 20 January 2012

Abstract Enzymes play a pivotal role in catalyzing diverse reactions. However, their instability upon repetitive/prolonged use, as well as their inhibition by high substrates and product concentration, remains an area of concern. In this study, porcine pancreatic α-amylase was immobilized on magnetic Fe_2O_3 nanoparticles (Fe_2O_3-NPs) in order to hydrolyze starch. The magnetic nanoparticle bound enzymes retained 94% of their initial enzyme activity. X-ray diffraction and atomic force microscopy analyses showed that the prepared matrix had advantageous microenvironment and a large surface area for binding significant amounts of protein. Functional groups present in enzyme and support were monitored by Fourier transform infrared spectroscopy. Immobilized enzyme exhibited lowered pH optimum (pH 6.0) to a greater degree than its soluble counterpart (pH 7.0). Optimum temperature for the immobilized enzyme shifted towards higher temperatures. The immobilized enzyme was significantly more resistant to inactivation caused by various metal ions and chemical denaturants. Immobilized α-amylase hydrolyzed 92% starch in a batch process, after 8 h at 40°C; while the free enzyme could hydrolyze only 73% starch under similar experimental conditions. A reusability experiment demonstrated that the immobilized enzyme retained 83% of its original activity even after its 8^{th} repeated use.

Keywords: α-Amylase, immobilization, nanoparticles, stabilization, starch hydrolysis

Mohammad Jahir Khan, Qayyum Husain
Department of Biochemistry, Faculty of Life Sciences, Aligarh Muslim University, Aligarh 202-002, India

Qayyum Husain*
Faculty of Applied Medical Sciences, Jazan University, Jazan, Saudi Arabia
Tel: 91-571-2700741; Fax: 91-571-2706002
E-mail: qayyumbiochem@gmail.com

Ameer Azam
Centre of Excellence in Material Science (Nanomaterials), Zakir Husain College of Engineering and Technology, Aligarh Muslim University, Aligarh 202-002, India

1. Introduction

The enzymes α-amylases (E.C. 3.2.1.1) catalyze the hydrolysis of α-1,4 glycosidic bonds present in starch, glycogen, and other related carbohydrates [1]. They are present in plants, animals, and microorganisms and have extensive applications in medicine, textiles, fermentation, and the food industry [2]. The exploitation of soluble enzymes in industries is limited due to product inhibition, instability, non-reusability, and difficult recovery from a reaction system [3]. In order to overcome these limitations, enzyme immobilization has been considered one of the best alternatives to using enzymes on a large scale, in industrial and environmental applications [4]. Immobilization also protects enzymes from denaturation and helps to retain them in biochemical reactors in order to further catalyze the subsequent feed and to offer more economical use of biocatalysts in industry, waste water treatment, and the development of bioprocess monitoring devices, such as biosensors [5,6].

In the recent past, nanosized materials have been widely employed for enzyme immobilization. Due to the large surface area of nanosized materials, they provide superior loading capacity and low mass transfer resistance [7,8]. The magnetic nanoparticles have now been used in conjunction with biological materials, such as proteins, enzymes, and nucleic acids, as they result in complete and easy recovery of these materials from reaction systems, thereby reducing the operational costs of the processes [9-

11].

In the present work, an attempt has been made to immobilize α-amylase on Fe_2O_3-NPs. The immobilized enzyme was characterized by X-ray diffraction (XRD), Fourier transform-infrared (FT-IR) spectroscopy, and atomic force microscopy (AFM). Thermal behavior of both soluble and immobilized α-amylase was studied by thermo-gravimetric (TGA) and differential thermal analysis (DTA). Effects of various metal ions and denaturing agents on the activity of soluble and immobilized α-amylase were monitored. Hydrolysis of starch by soluble and immobilized enzymes was performed in batch processes. The reusability of the immobilized enzyme was also examined.

2. Materials and Methods

2.1. Materials

Materials used included α-Amylase (Porcine pancreas), starch, maltose, glucose and 3,5 dinitro-salicylic acid (DNS); these were purchased from SRL Chemicals (Mumbai, India). Ferric nitrate, mono hydrated citric acid, and metal ions were obtained from Sigma-Aldrich Co. (USA). All other chemicals and reagents were of analytical grade and were used without further purification.

2.2. Synthesis of Fe_2O_3-NP by sol-gel method

Ferric oxide nanoparticles (Fe_2O_3-NPs) were synthesized according to the procedure described by Raming et al, with several modifications [12]. Ferric nitrate (200 mL, 0.1 M) was used as a precursor solution and was gelated with 800 mL of mono hydrated citric acid (0.05 ~ 0.2 M); as ligand and triple distilled water were used as solvents. Ferric nitrate was added, dropwise, to the citric acid solution; it was vigorously shaken. The solution was heated, at 70°C, with continuous stirring until the gel was formed and the water was completely evaporated. The dried gel was then annealed at 100°C for 16 h in order to solidify the gel, which was grounded for 30 min. The formed Fe_2O_3-NP was used for further studies.

2.3. XRD analysis of Fe_2O_3-NP and Fe_2O_3-NP adsorbed α-amylase

The crystal structure of Fe_2O_3-NP and Fe_2O_3-NP, which adsorbed the α-amylase, was obtained with an X-ray diffractometer (Rigaku Miniflex X-ray diffractometer), using a monochromatized X-ray beam with nickel-filtered Cu Kα radiation. A continuous scan mode was used to collect 2 θ data from 5° to 80°. The particle size (D) of the samples was determined by Scherer's formula as:

$$D = 0.9\ \lambda/B \cos\theta$$

where λ is the X-ray wavelength (1.54060 Å), B is the full width at half-maximum of Fe_2O_3 (400) line, and θ is the diffraction angle.

2.4. Immobilization of α-amylase

Fe_2O_3-NP (40 mg) was added to α-amylase (2,083 U), and this mixture was stirred overnight in 0.1 M sodium phosphate buffer, pH 7.0 at 4°C. The enzyme bound on nano-support was collected by centrifugation at 5,000 × *g* for 10 min at 4°C. The unbound enzyme was removed by washing it three times, with a 0.1 M sodium phosphate buffer, pH 7.0. The immobilized enzyme was stored in an assay buffer at 4°C for further use.

2.5. AFM analysis

The tapping mode AFM experiment of free nanoparticles and enzyme bound nanoparticles was performed using commercial etched silicon tips as an AFM probe, with a characteristic resonance frequency of ca. 300 Hz (RTESP, Veeco). The samples were placed, dropwise, on a mica wafer, air dried at room temperature for 12 h, and the images were recorded with a Veeco Innova nanoscope II AFM. Microscopic scans were carried out on several surface positions in order to check the surface uniformity.

2.6. FT-IR analysis of enzyme, Fe_2O_3-NP and Fe_2O_3-NP adsorbed α-amylase

The FT-IR spectra of the enzyme, Fe_2O_3-NP and Fe_2O_3-NP, adsorbed α-amylase; these were recorded through the potassium bromide pellet method on INTERSPEC 2020 (USA) in the range of 400 ~ 4,000/cm. The calibration was performed by polystyrene film. Samples were injected with a Hamiet 100 μL syringe in an ATR box. The syringe was washed with acetone; this was followed by distilled water. FT-IR analysis was performed in order to examine the functional groups present in the enzyme and support.

2.7. Thermogravimetric and differential thermal analysis

TGA was performed using a Mettler-3000 thermal analyzer with a 2.0 mg sample, with heating rate of 10°C/min in N_2 atmosphere. DTA analysis was also carried out in a similar heating range, using TA-DSC, Q 200 (USA).

2.8. Effect of pH and temperature

Enzyme activity of soluble and immobilized α-amylase (51.0 U) was assayed in the buffers of different pHs (4.0 ~ 8.0). The buffers used were sodium acetate (pH 4.0, 5.0), sodium phosphate (pH 6.0, 7.0), and Tris-HCl (pH 8.0). The molarity of each buffer was 0.1 M. The activity at pH 7.0 and pH 6.0 were taken as control (100%) for the calculation of the remaining percentage of activity for the soluble and immobilized enzymes, respectively.

The activity of soluble and immobilized α-amylase (51.0 U) was measured at various temperatures (20 ~ 80ºC). Enzyme activity at 40 and 50ºC was taken as control (100%) for the calculation of the remaining percentage of activity for the soluble and immobilized enzymes, respectively.

2.9. Effect of metal ions on activity of soluble and immobilized α-amylase

Soluble and immobilized α-amylase (51.0 U) was independently incubated, with a 5.0 mM solution of metal ions (chlorides of Na^+, K^+, Mg^{2+}, Cu^{2+}, Co^{2+}, Ba^{2+}, Zn^{2+}, Ca^{2+}, and Fe^{3+}); their activity was determined in a 0.1 M sodium phosphate buffer, pH 7.0 at 40ºC. The activity of enzymes in the absence of metal ions was taken as control (100%) for the calculation of the remaining percentage of the activity for the soluble and immobilized enzymes.

2.10. Effect of urea on activity of soluble and immobilized α-amylase

Soluble and immobilized α-amylase (51.0 U) was incubated with a 4.0 M urea for different time intervals. The enzyme activity without urea was taken as control (100%) for the calculation of the remaining percentage activity for the soluble and immobilized enzymes.

2.11. Reusability of immobilized α-amylase

Immobilized α-amylase (51.0 U) was taken in triplicates in order to assay its activity. After each assay, the immobilized enzyme was taken out from assay tubes and stored in a 0.1 M sodium phosphate buffer, pH 7.0 at 4°C. This procedure was repeated for eight consecutive days. The activity determined on first day was considered as the control (100%) for the calculation of the remaining percentage activity after each use.

2.12. Hydrolysis of starch in batch process

Starch solution (1.0%, w/v) was incubated independently, with soluble and immobilized α-amylase (4,850 U) at 40ºC with constant stirring for 8 h. The aliquots (500 µL) were taken out at indicated time intervals, hydrolysis of starch and the formation of maltose was assayed by the DNS method [13].

2.13. Activity assay for α-amylase

The activity of α-amylase was assayed by the DNS method [13], using a 1.0% soluble starch as a substrate. The enzyme in a 0.1 M sodium phosphate buffer, pH 7.0 (250 µL) and starch (250 µL), was incubated for 30 min at 40°C. The reaction was stopped by adding 1.5 mL DNS reagent and heating the solution in boiling water for 5 min. DNS is a coloured reagent, and the reducing groups released from starch by α-amylase action were measured by the reduction of this reagent. After cooling, 1.5 mL of distilled water was added and, finally, absorbance was recorded spectrophotometrically, at 540 nm.

One unit (1.0 U) of α-amylase activity is defined as the amount of enzyme that liberates 1.0 µM of maltose per min, under standard assay conditions. A standard curve of absorbance against the amount of maltose was prepared to calculate the amount of maltose released during assay.

2.14. Estimation of protein

Protein concentration was determined by a dye binding method [14]. Bovine serum albumin was used as a standard protein.

2.15. Statistical analysis

Each value represents the mean for three independent experiments performed in duplicates, with average SDs of < 5%. Data were analyzed by one-way ANOVA, and *p*-values of < 0.05 were considered statistically significant.

3. Results and Discussion

3.1. Immobilization efficiency of α-amylase

Several methods have previously been employed for the immobilization of α-amylase. Among these methods, physical adsorption onto insoluble materials has been considered one of the preferred choices, due to its simplicity and regeneration of support. Moreover, this method of enzyme immobilization does not require pre-activation steps for support [15].

Table 1 demonstrates the immobilization efficiency of α-amylase. Fe_2O_3-NP adsorbed α-amylase preserved 94% of its initial enzyme activity which was higher compared to previous reported immobilization studies [16,17].

3.2. XRD analysis

Table 1. α-amylase immobilized on Fe_2O_3-NP

Enzyme loaded (X) (U)	Enzyme activity in washes (Y) (U)	Activity bound to Fe_2O_3-NP (U)			Activity yield (%) (B/A × 100)
		Theoretical (X-Y=A)	Actual (B)	Effectiveness factor (B/A) = (η)	
2,083	1,528	554	521	0.94	94

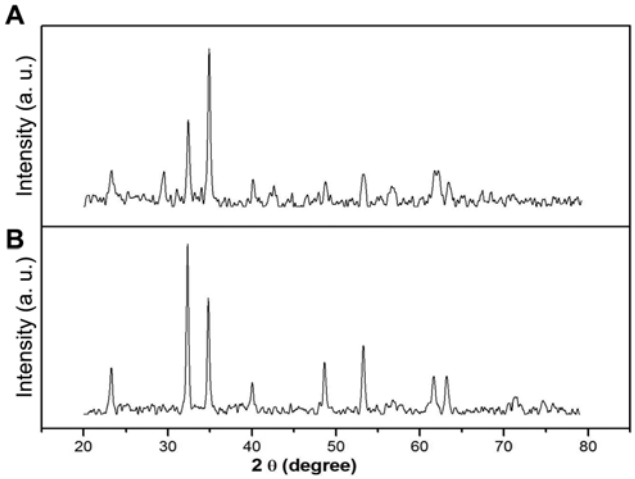

Fig. 1. XRD analysis of Fe_2O_3-NP and Fe_2O_3-NP adsorbed α-amylase. XRD analysis of Fe_2O_3-NP (A) and Fe_2O_3-NP adsorbed α-amylase (B) was obtained with an X-ray diffractometer (Rigaku Miniflex X-ray diffractometer) using a monochromatized X-ray beam with nickel-filtered Cu Kα radiation, in the range of $5^o \sim 80^o$.

The diffraction patterns of Fe_2O_3-NP and Fe_2O_3-NP adsorbed α-amylase are represented in Fig. 1. The results showed that nanoparticles have hexagonal crystal symmetry with an average crystalline size of 26.90 nm (Fig. 1A), which was decreased to 24.25 nm (Fig. 1B) after enzyme adsorption. The intensity peaks of the NPs were masked after immobilization as the enzyme covered significant parts of the NP surfaces [18]. The binding of magnetic nanoparticles to bioactive substances involved a number of interactions, including interactions between organic ligands and those between amino acid side chains of protein and metal centers. This might be accredited better enzyme-substrate interactions on immobilization, with the availability of larger surface areas on nanoparticle and possible structural modulation or better exposure of the active site [19]. Moreover, such coupling of biomolecular entities with nanoparticles provides enhanced thermal stability of the enzyme, allowing its use in various analytical, biotechnological, and industrial applications [20].

3.3. AFM and FT-IR analysis

Morphological information presents a physical picture of how α-amylase molecules are assembled on nanoparticle surfaces (Fig. 2). The roughness shown in these images can also be analyzed and related to the pattern of immobilization. We used the peak-to-valley distance in these images as an indicator of surface roughness. As shown (Fig. 2A), the nanoparticle surface is relatively smooth and has small peak-to-valley distance. Once an enzyme molecule is adsorbed (Fig. 2B), there was a significant increment in peak-to-valley distance. Thus, we can conclude that nanoparticle surfaces were fully covered with enzymes after immobilization, which corresponds to high enzyme loading [21,22].

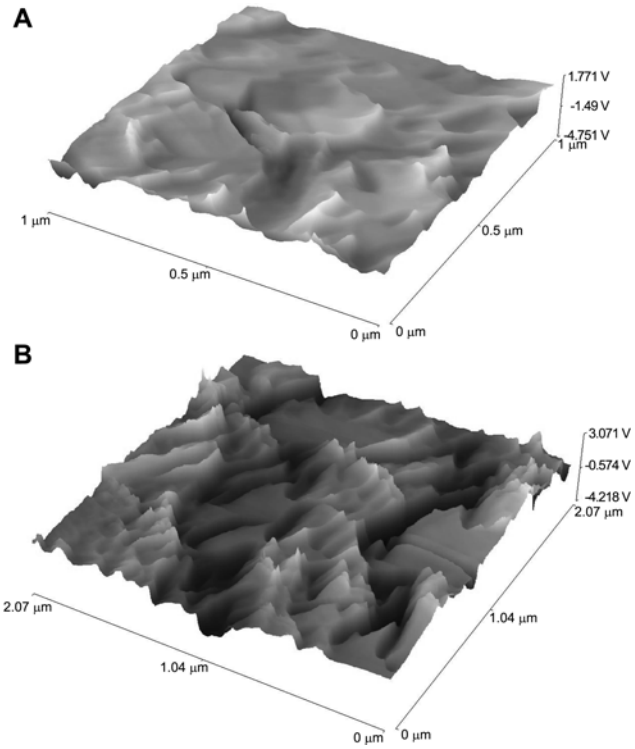

Fig. 2. Atomic force microscopy of Fe_2O_3-NP and Fe_2O_3-NP adsorbed α-amylase. Tapping mode AFM experiments were performed using commercial etched silicon tips as AFM probes with typical resonance frequencies of ca. 300 Hz. Atomic force micrographs for Fe_2O_3-NP (A) and Fe_2O_3-NP adsorbed α-amylase (B) have been shown.

Fig. 3 shows FT-IR spectra of Fe_2O_3-NP, α-amylase and Fe_2O_3-NP adsorbed α-amylase. FT-IR spectroscopy revealed that the formation of hydrogen bonds between amino groups and water may result in tremendous water solubility, which makes them ideal for enzyme immobilization [23]. A sharp peak was observed at 538/cm (Figs. 3A and 3C), which is characteristic of Fe-O vibrations. The amide I peak appeared between 1,600 and 1,700/cm due to C=O stretching vibrations of the protein backbone. This peak is sensitive to short range, imposed by distinct hydrogen bonding arrangements in the secondary structure of the proteins [24]. The peak at 1,108/cm (Fig. 3B) is most likely reflecting an imidazole ring of the histidine side chain. The interactions of NPs with C-N groups of enzymes were also evident with the shifting of the amide A band from 3,341/cm toward ahigher frequency, 3,349/cm (Figs. 3B and 3C) [25].

3.4. TGA and DTA analysis

TGA and DTA results of free and Fe_2O_3-NP bound α-amylase are shown in Fig. 4. The TGA spectra of enzyme showed a 5% loss in weight at 200°C, followed by a sharp

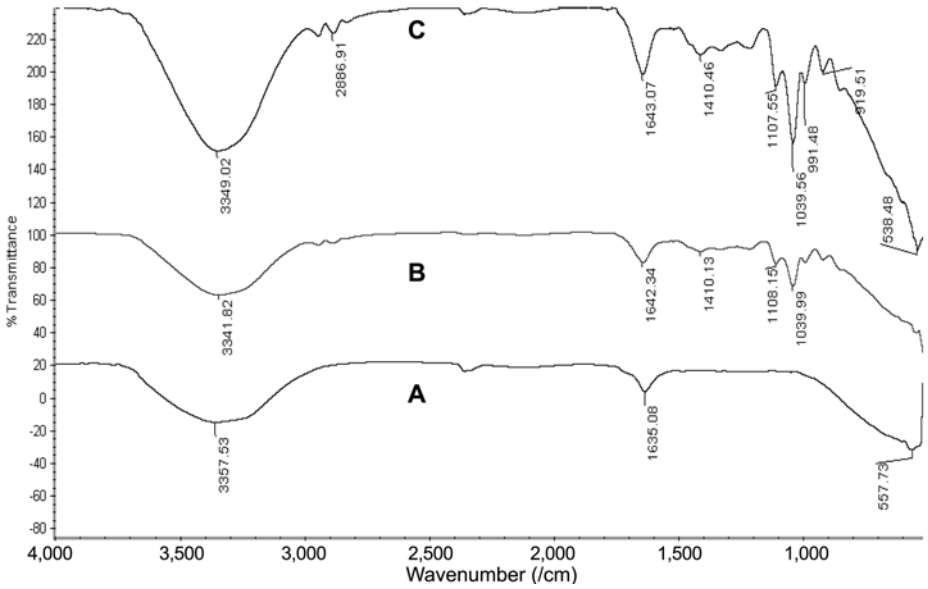

Fig. 3. FT-IR spectra of Fe_2O_3-NP, α-amylase, and Fe_2O_3-NP adsorbed α-amylase. FT-IR analysis was performed to monitor the interactions between enzymes and nanoparticles. FT-IR spectra of Fe_2O_3-NP (A), α-amylase (B), and Fe_2O_3-NP adsorbed α-amylase (C) were monitored with INTERSPEC 2020 (USA) in the range of 400 ~ 4,000/cm.

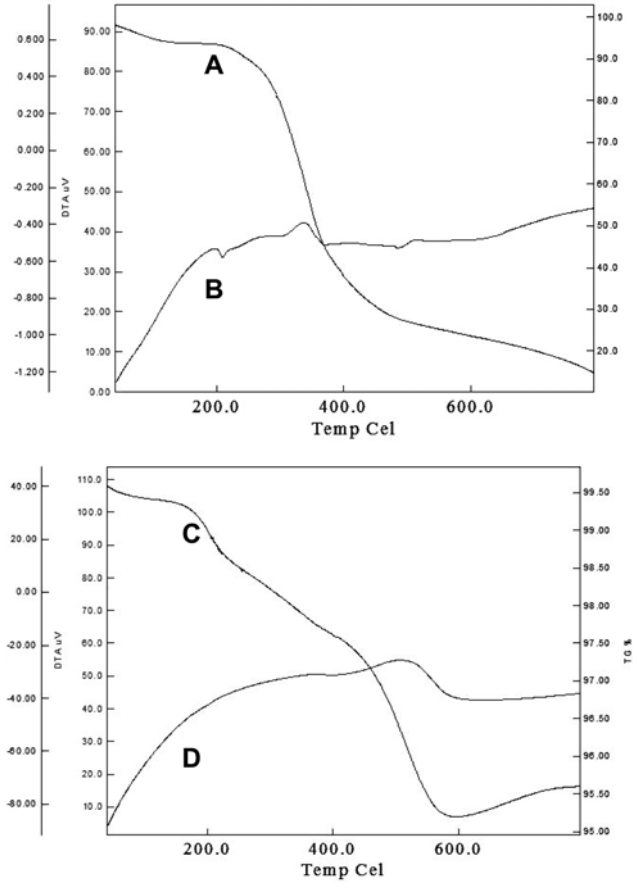

Fig. 4. Thermogravimetric and differential thermal analysis of α-amylase and Fe_2O_3-NP adsorbed α-amylase. Fig. 4 shows a thermogravimetric analysis of α-amylase (A) and Fe_2O_3-NP adsorbed α-amylase (C). The differential thermal analysis of α-amylase (B) and Fe_2O_3-NP adsorbed α-amylase has been shown in (D).

peak at 400°C; this indicates a weight loss of over 65% (Fig. 4A). However, Fe_2O_3-NP adsorbed α-amylase exhibited very slight (5%) weight loss (Fig. 4C) under a similar temperature range. The significant weight loss in the free enzyme might be due to the removal of free and bound water and solvent.

The DTA curve showed that thermal decomposition of enzymes begins at 180°C (Fig. 4B) while Fe_2O_3-NP adsorbed α-amylase retained a significantly higher stability of up to 300°C (Fig. 4D). This showed that the immobilized enzyme preparation can be employed at a higher temperature for various applications.

3.5. Effect of pH and temperature

The pH optimum for soluble enzymes was found at pH 7.0, which shifted to pH 6.0 upon immobilization (Fig. 5). A shift in pH optimum upon immobilization depends on enzyme microenvironment as well as the structure and charge of the matrix [26]. The change in pH optimum for immobilized α-amylase has also been reported by several earlier investigators [27,28].

The temperature optimum for α-amylase shifted from 40 to 50°C after immobilization (Fig. 6). However, as the temperature increased, activity of free enzymes decreased more rapidly, compared with the immobilized counterpart. The inability of a free enzyme to enhance its thermal stability is one of the major limitations for its application in continuous reactors. An increase in temperature optimum of immobilized enzymes revealed that the enzyme might be more rigid to structural changes induced by heat [29,30].

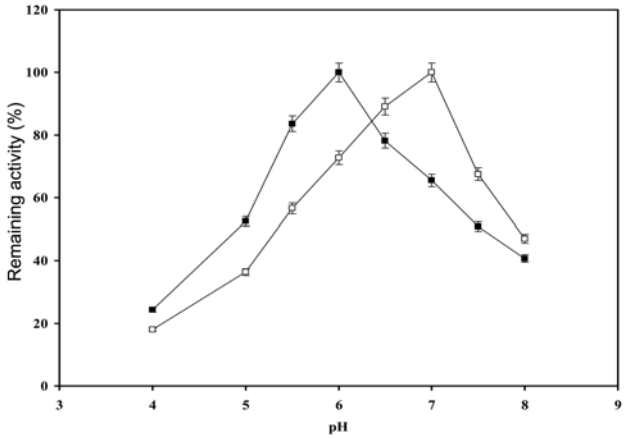

Fig. 5. pH activity profiles for soluble and immobilized α-amylase. The enzyme activity of soluble and immobilized α-amylase (51.0 U) was measured in the buffers of various pHs. The buffers used were: sodium acetate (pH 4.0, 5.0), sodium phosphate (pH 6.0, 7.0), and Tris-HCl (pH 8.0). The molarity of each buffer was 0.1 M. The activity at pH 7.0 and pH 6.0 were taken as controls (100%) for the calculation of remaining percent activity for soluble and immobilized α-amylase, respectively. The symbols show (-□-) soluble and (-■-) immobilized α-amylase.

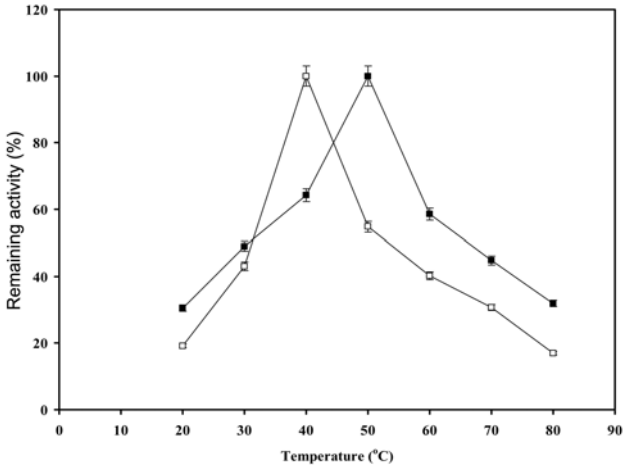

Fig. 6. Temperature activity profiles for soluble and immobilized α-amylse. The activity of soluble and immobilized α-amylase (51.0 U) was measured at various temperatures (20 ~ 80°C) for 30 min. The enzyme activity at 40 and 50°C was taken as control (100%) for the calculation of remaining percent activity for the soluble and immobilized enzymes, respectively. For symbols, please refer to figure legend 5.

3.6. Effect of metal ions

Our studies showed that the activity of immobilized enzymes was less affected in the presence of various metal ions, compared with free enzymes (Table 2). However, we observed that Cu^{++} caused maximum inhibition in the activity of both free and immobilized enzymes [31]. The relative activity of the immobilized α-amylase was higher than that of the soluble enzyme in the presence of NaCl, KCl, $CaCl_2$, and $CoCl_2$ [32].

Table 2. Effect of metal ions on soluble and immobilized α-amylase

Metal ions (5.0 mM)	Remaining activity (%)*	Immobilized enzyme
	Soluble enzyme	
None	100	100
NaCl	106.9 ± 2.90	118.1 ± 1.71
KCl	103.6 ± 1.11	110.5 ± 2.51
$MgCl_2$	96.3 ± 0.97	97.6 ± 2.85
$CuCl_2$	21.7 ± 2.00	35.7 ± 2.37
$CoCl_2$	81.4 ± 1.94	114.7 ± 1.43
$BaCl_2$	112.2 ± 2.54	91.4 ± 1.65
$ZnCl_2$	53.0 ± 1.27	77.6 ± 1.25
$CaCl_2$	97.5 ± 1.11	105.7 ± 0.95
$FeCl_3$	63.1 ± 2.46	92.3 ± 1.69

*The percent activity of an enzyme compared with the activity without the presence of metal ions.

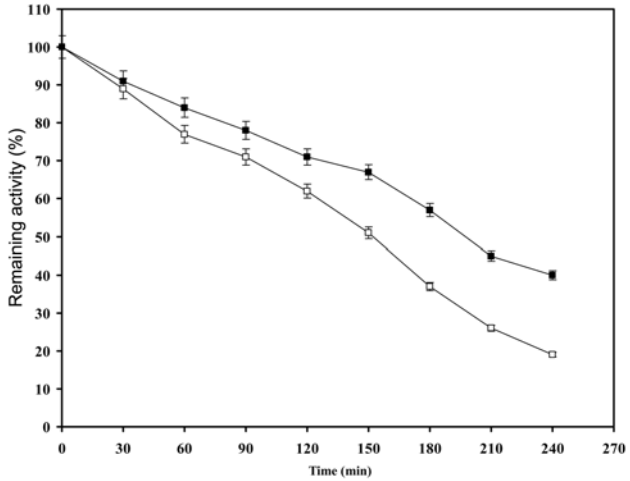

Fig. 7. Effect of 4.0 M urea on soluble and immobilized α-amylase. Soluble and immobilized α-amylase (51.0 U) was incubated with 4.0 M urea, in a 0.1 M sodium phosphate buffer, pH 7.0. Enzyme activity was determined at different time intervals under conditions mentioned in the text. To calculatethe remaining percent activity, untreated samples were considered as controls (100%). For symbols, please refer to figure legend 5.

3.7. Effect of urea

The immobilized α-amylase was more stable than the soluble enzyme upon exposure to 4.0 M urea for a longer duration (Fig. 7). The result showed an 81% loss in enzyme activity for soluble enzymes, while the immobilized enzyme retained more than 40% with identical exposure. Earlier studies have indicated that proteins become unfolded due to direct interaction of urea molecules with the peptide backbone, via hydrogen bonding or hydrophobic interactions [33]. Molecular crowding/confinement theory has predicted that Fe_2O_3-NPs provide a beneficial confined space that resists conformational changes to the immobilized enzyme, even at higher concentration of urea [34].

Table 3. Hydrolysis of starch by soluble and immobilized α-amylase in batch processes at 40°C

Time (min)	Remaining activity (%)	
	Soluble	Immobilized
0	ND	ND
30	14 ± 0.69	9 ± 1.39
60	20 ± 2.11	15 ± 1.42
90	25 ± 1.34	20 ± 2.48
120	36 ± 2.08	42 ± 0.99
180	47 ± 1.22	59 ± 2.22
240	61 ± 1.34	68 ± 1.90
300	67 ± 0.98	74 ± 1.10
360	73 ± 1.75	83 ± 0.79
420	73 ± 1.11	92 ± 1.15
480	73 ± 2.43	92 ± 1.42

ND: Not determined.

3.8. Hydrolysis of starch in batch processes by soluble and immobilized α-amylase

Table 3 describes the hydrolysis of starch by the soluble and immobilized α-amylase for various time intervals at 40°C. The soluble and immobilized enzymes hydrolyzed 61 and 68% starch after 4 h of incubation, respectively. Additionally, the maximum hydrolysis of starch, 74% by the free enzyme, was attained after 8 h, while the immobilized enzyme hydrolyzed a higher concentration of starch (92%) under similar incubation time. This was due to the fact that the soluble enzyme was more accessible to the substrate for first few hours but, after a prolonged period of time, the rate of hydrolysis decreased more quickly. This might be due to the enzyme unfolding or the inhibition of enzyme activity by its own product [35,36]. Satish *et al.* reported similar results, where starch was hydrolyzed by α-amylase immobilized on super porous cellulose beads [37].

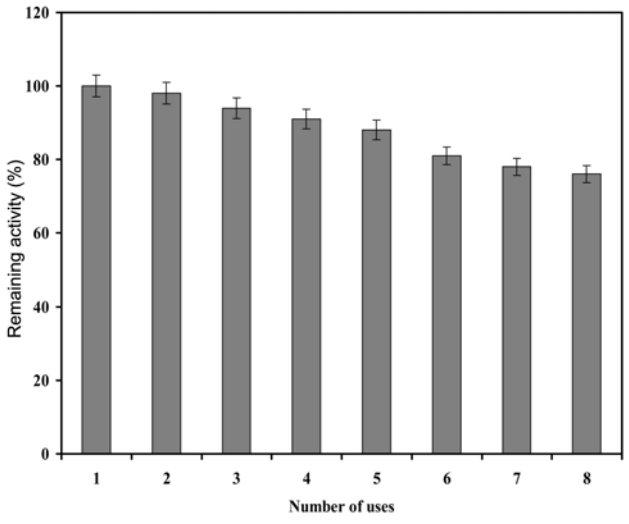

Fig. 8. Reusability of immobilized α-amylase. The reusability of immobilized α-amylase was monitored for 8 successive days. The preparation was taken in triplicates and assayed for the remaining percentage activity. The activity determined on the first day was taken as the control (100%) for the calculation of the remaining percentage activity after each use.

3.9. Reusability

Enzymes are quite expensive products, so reusability and operational stability are important criteria for enzyme application at the industrial level. Immobilized α-amylase showed 83% residual activity even after the 8th consecutive use (Fig. 8). The significant retention in immobilized enzyme activity on repeated uses might be due to the multipoint non-covalent attachment of the enzyme to nanosupport.

4. Conclusion

In this study, α-amylase was immobilized onto Fe_2O_3-NPs by a simple adsorption mechanism with excellent catalytic efficiency. Immobilized α-amylase was found to be stable against various types of physical and chemical denaturants. The increased temperature optimum of immobilized enzyme results in several benefits; higher temperature decreased the viscosity of both substrate and product, increased the reaction rate with less operational time, and minimized the risk of microbial contamination. Reusability experiments further supported that the adsorbed enzyme did not detach from the nanosupport with repeated use and, therefore, such preparations could be considered for the continuous hydrolysis of starch for longer durations, even at higher temperatures. Thus, such immobilized enzymes could prove useful for the efficient conversion of starch in continuous reactors at the industrial level.

Acknowledgement

Aligarh Muslim University, Aligarh is gratefully acknowledged for providing UGC, scholarship to one of us (M. J. Khan).

Nomenclature

AFM : Atomic force microscopy
DNS : 3,5 Dinitro-salicylic acid
DTA : Differential thermal analysis
FT-IR : Fourier transform-infrared spectroscopy
NPs : Nanoparticles
TGA : Thermo-gravimetric analysis
XRD : X-ray diffraction

References

1. Bordbar, A. K., K. Omidiyan, and R. Hosseinzadeh (2005) Study on interaction of α-amylase from *Bacillus subtilis* with cetyl trimethyl ammonium bromide. *Colloid. Surf. B: Bioint.* 40: 67-71.
2. Abd El-Ghaffar, M. A. and M. S. Hashem (2009) Immobilization of α-amylase onto chitosan and its amino acid condensation adducts. *J. Appl. Polym. Sci.* 112: 805-814.
3. Akoh, C. C., S. W. Chang, G. C. Lee, and J. F. Shaw (2008) Biocatalysis for the production of industrial products and functional foods from rice and other agricultural produce. *J. Agric. Food Chem.* 56: 10445-104451.
4. Husain, Q. (2010) β Galactosidases and their potential applications. *Crit. Rev. Biotechnol.* 30: 41-62.
5. Husain, Q. (2006) Potential applications of the oxidoreductive enzymes in the decolorization and detoxification of textile and other synthetic dyes from polluted water: A review. *Crit. Rev. Biotechnol*. 26: 201-221.
6. Mateo, C., O. Abian, R. Fernandez-Lafuente, and J. M. Guisan (2000) Increase in conformational stability of enzymes immobilized on epoxy-activated supports by favoring additional multipoint covalent attachment. *Enz. Microb. Technol.* 26: 509-515.
7. Chen, B., M. E. Miller, and R. A. Gross (2007) Effects of porous polystyrene resin parameters on *Candida antarctica* lipase B adsorption, distribution, and polyester synthesis activity. *Langmuir* 23: 6467-6474.
8. Kim, M. I., J. Kim, J. Lee, and H. Jia (2007) Crosslinked enzyme aggregates in hierarchically-ordered mesoporous silica: A simple and effective method for enzyme stabilization. *Biotechnol. Bioeng.* 96: 210-218.
9. Safarik, I. and M. Safarikova (2009) Magnetic nano and microparticles in biotechnology. *Chem. Pap.* 63: 497-505.
10. Safarikova, M., L. Ptackova, I. Kibrikova, and I. Safarık (2005) Biosorption of water-soluble dyes on magnetically modified *Saccharomyces cerevisiae* subsp. *uvarum* cells. *Chemosphere* 59: 831-835.
11. Namdeo, M. and S. K. Bajpai (2009) Immobilization of α-amylase onto cellulose-coated magnetite (CCM) nanoparticles and preliminary starch degradation study. *J. Mol. Catal. B: Enzym.* 59: 134-139.
12. Raming, T. P., A. J. Winnubst, C. M. van Kats, and A. P. Philipse (2002) The synthesis and magnetic properties of nanosized hematite (α-Fe_2O_3) particles. *J. Colloid Int. Sci.* 249: 346-350.
13. Bernfield, P. (1955) Amylases α and β. pp. 149-158. In: S. P. Colowick and N. O. Kaplan (eds.). *Methods in enzymol*. Academic press, NY.
14. Bradford, M. M. (1976) Rapid and sensitive method for quantitation of microgram quantities of protein utilizing principle of protein-dye binding. *Anal. Biochem.* 72: 248-254.
15. Iyer, P. V. and L. Ananthanarayan (2008) Enzyme stability and stabilization-aqueous and non-aqueous environment. *Proc. Biochem.* 43: 1019-132.
16. Kennedy, J. F. and M. Paterson (1993) Application of cellulosic fast flow column filters to protein immobilization and recovery. *Polym. Int.* 32: 71-81.
17. Hasirci, N., S. Aksoy, and H. Tumturk (2006) Activation of poly (dimmer acid-co-alkyl polyamine) particles for covalent immobilization of α-amylase. *Reac. Func. Polym.* 66: 1546-1551.
18. Mallikarjuna, N. N., S. K. Manohar, P. V. Kulkarni, A. Venkataraman, and T. M. Aminabhavi (2005) Novel high dielectric constant nanocomposites of polyaniline dispersed with γ-Fe_2O_3 nanoparticles. *J. Appl. Polym. Sci.* 97: 1868-1874.
19. Weng, L., L. Zhang, D. Ruan, L. Shi, and J. Xu (2004) Thermal gelation of cellulose in a NaOH/thiourea aqueous solution. *Langmuir* 20: 2086-2093.
20. Konwarh, R., N. Karak, S. K. Rai, and A. K. Mukherjee (2009) Polymer-assisted iron oxide magnetic nanoparticle immobilized keratinase. *Nanotechnol.* 20: 225107-225117.
21. Scaramuzzo, F. A., R. Salvati, B. Paci, A. Generosi, V. Rossi-Albertini, A. Latini, and M. Barteri (2009) Nanoscale in situ morphological study of proteins immobilized on gold thin films. *J. Phys. Chem. B.* 113: 15895-15899.
22. Saal, K., V. Sammelselg, A. Lohmus, E. Kuusk, G. Raidaru, T. Rinken, and A. Rinken (2002) Characterization of glucose oxidase immobilization onto mica carrier by atomic force microscopy and kinetic studies. *Biomol. Eng.* 19: 195-199.
23. Lei, C. H., Y. Shin, J. Liu, and E. J. Ackerman (2002) Entrapping enzyme in a functionalized nanoporous support. *J. Am. Chem. Soc.* 124: 11242-11243.
24. Jackson, M. and H. H. Mantsch (1995) The use and misuse of FTIR spectroscopy in the determination of protein structure. *Crit. Rev. Biochem. Mol. Biol.* 30: 95-120.
25. Krimm, S. and J. Bandekar (1986) Vibrational spectroscopy and conformation of peptides, polypeptides and proteins. *Adv. Protein Chem.* 38: 181-364.
26. Roig, M. G, A. Slade, and J. F. Kennedy (1993) α-Amylase immobilized on plastic supports: Stabilities, pH and temperature profiles and kinetic parameters. *Biomat. Artif. Cells Immob. Biotechnol.* 21: 487-525.
27. Bayramoglu, G., M. Yilmaz, and M. Y. Arica (2004) Immobilization of thermostable α-amylase onto reactive membranes: Kinetics characterization and application to continuous starch hydrolysis. *Food Chem.* 84: 591-599.
28. Arica, M. Y., V. Hasirci, and N. G. Alaeddinoglu (1995) Covalent immobilization of α-amylase onto pHEMA microspheres: Preparation and application to fixed bed reactor. *Biomaterials* 16: 761-768.
29. Magri, M. L., M. V. Miranda, and O. Cascone (2005) Immobilization of soybean seed coat peroxidase on polyaniline: Synthesis optimization and catalytic properties. *Biocatal. Biotrans.* 23: 339-346.
30. Lee, P. M., K. H. Lee, and S. Y. Siaw (1993) Covalent immobilization of aminoacrylase to alginate for L-phenylalanine production. *J. Chem. Technol. Biotechnol.* 58: 65-70.
31. Ramesh, M. V. and B. K. Lonsane (1990) Effect of metal salts and protein modifying agents on activity of thermostable α-amylase produced by *Bacillus lichiniformis* M27 under solid state fermentation. *Chem. Microb. Technol. Lebensm.* 12: 129-136.
32. Lo, H., L. Lin, H. Chen, W. Hsu, and C. Chang (2001) Enzymatic properties of a SDS-resistant *Bacillus* sp. TS-23 α-amylase produced by recombinant *Escherichia coli*. *Proc. Biochem.* 36: 743-750.
33. Makhatadze, G. I. and P. L. Privalov (1992) Protein interactions with urea and guanidinium chloride. A calorimetric study. *J. Mol. Biol.* 226: 491-505.
34. Zhou, H. X. (2004) Protein folding and binding in confined spaces and in crowded solutions. *J. Mol. Recognit.* 17: 368-375.
35. Tanriseven, A. and S. Dogan (2002) A novel method for the immobilization of β-galactosidase. *Proc. Biochem*. 38: 27-30.
36. Yagar, H., F. Ertan, and B. Balkan (2008) Comparison of some properties of free and immobilized α-amylase by *Aspergillus sclerotiorum* in calcium alginate gel beads. *Prep. Biochem. Biotechnol.* 38: 13-23.
37. Shewale, S. D. and A. B. Pandit (2007) Hydrolysis of soluble starch using *Bacillus licheniformis* α-amylase immobilized on superporous CELBEADS. *Carbohyd. Res.* 342: 997-1008.